Biophysical Journal Volume: 00 Month Year 1–8

Shape transformations of lipid bilayers following rapid cholesterol uptake

M. Rahimi, D. Regan, M. Arroyo, A.B. Subramaniam, H.A. Stone, M. Staykova

Abstract

High cholesterol levels in the blood increase the risk of atherosclerosis. A common explanation is that the cholesterol increase in the plasma membrane perturbs the shape and functions of cells by disrupting the cell signalling pathways and the formation of membrane rafts. In this work, we show that following enhanced transient uptake of cholesterol, mono-component lipid bilayers change their shape similarly to cell membranes *in vivo*. The bilayers either expel lipid protrusions or spread laterally as a result of the ensuing changes in their lipid density, the mechanical constraints imposed on them, and the properties of cyclodextrin used as a cholesterol donor. In light of the increasingly recognized link between the membrane tension and cell behavior, we propose that the physical adaptation of the plasma membrane to the cholesterol uptake may play a substantial role in the biological response.

Submitted October 17, 2016

*Correspondence:
Editor:

INTRODUCTION

Cholesterol is a common constituent of mammalian cell membranes and a major regulator of their function. In healthy cells, it accounts for 25-30% of the lipid content of the plasma membrane (1). Cholesterol content in cells is biologically regulated through various processes. Cells can synthesize cholesterol or acquire it exogeneously from low-density lipoproteins (LDL). When in surplus, cholesterol is donated to extracellular receptors or transported to the endoplasmic reticulum for esterification and storage in cytoplasmic lipid droplets (2). Enhanced dietary uptake of cholesterol or disturbances in its trafficking have been associated with the development of pathological atherosclerotic lesions, which may reduce and even block the arterial blood flow (3, 4). At the cellular level, increased cholesterol content in the membrane can lead to cell spreading, formation of protrusions, loss of mobility and, eventually, cell death (5–7).

The cellular and molecular mechanisms underlying these disorders remain insufficiently understood, and are generally thought to depend on the interference of cholesterol with the membrane's lateral organization and cell signaling. Cholesterol is known to enter into stoichiometric complexes with certain phospholipids, thus forming cholesterol-rich membrane phases (8, 9). In vitro experiments on cells suggest that disrupting the lateral lipid organization by altering the level of cholesterol affects signal transduction and cytoskeletal dynamics (6, 7, 10, 11). Furthermore, high cholesterol levels induce the formation of membrane crystalline domains, which nucleate injurious cholesterol crystals (12) or globally increase the rigidity of the lipid membrane, thus inhibiting the function of certain transmembrane proteins (3).

While the resulting interference of cholesterol with cellular lipids and proteins has received considerable research attention, how membranes dynamically respond to rapid cholesterol uptake in the first place has never been examined. Yet, the cholesterol content of plasma membranes can increase by up to 3-fold within minutes following incubation of cells with cholesterol-loaded cyclodextrins (MβCD-Chol) (13, 14). An increase of similar rate and magnitude is observed in cells following endocytosis of LDLs (15–17), or more significantly in the early stages of atherosclerosis, when macrophages are known to hydrolyse the LDL aggregates in the extracellular matrix and absorb the released cholesterol (5, 6).

In this study, we track the dynamics of model membranes upon fast cholesterol delivery by MβCD-Chol at biologically relevant concentrations. We consider three different model membrane systems: 1) laterally unconstrained patches of supported lipid bilayers (SLB patches) obtained by fusing giant unilamellar vesicles to the supporting substrate, 2) continuous supported lipid bilayers (CSLB) that cover the whole substrate area, and 3) suspended giant unilamellar vesicles (GUVs)

0006-3495/08/09/2624/12 $2.00

(Fig. 1). We observe and rationalize a variety of in- and out-of-plane membrane transformations that depend on the mechanical constraints of the various membrane systems and on the properties of the cholesterol donor. Our results suggest a purely physical mechanism for some of the observed cellular behaviors upon uptake of cholesterol that complements our understanding of the biological mechanisms of atherosclerosis.

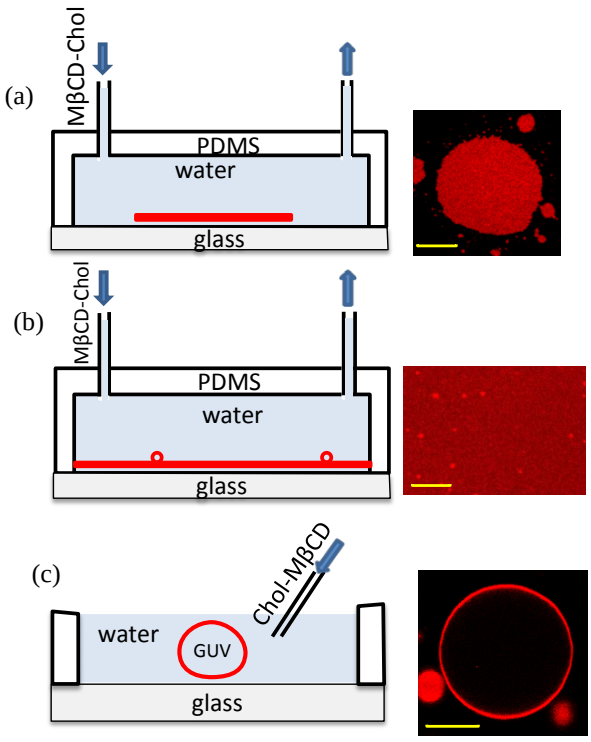

Figure 1: Membrane model systems and respective experimental setups: (a) SLB patch and (b) CSLB formed at the bottom glass of a microchannel that can be flushed with the solution of interest. Images are taken at the substrate plane. (c) GUVs, mixed with the desired solution in an open chamber and imaged at their equatorial plane. Scale bar 10 µm.

MATERIALS AND METHODS

DOPC (1,2-dioleoyl-sn-glycero-3-phosphocholine), Rh-DPPE (1,2-dipalmitoyl-sn-glycero-3-phosphoethanolamine-*N*-(lissamine rhodamine-B sulphonyl) (ammonium salt)) were purchased from Avanti Polar Lipids, and chloroform, trizma hydrichloride (Tris.HCl), sucrose, Methyl-β-cyclodextrin (MβCD), and cholesterol-chelated methyl-β-cyclodextrin (MβCD-Chol), also known as cholesterol water soluble, were purchased from Sigma Aldrich. All materials were used without further purification. Polydimethylsiloxane (PDMS) and curing agent were purchased from Dow Corning (Sylgard 184 Silicone Elastomer Kit).

Model membrane systems

GUVs were prepared from a 4 mM lipid-chloroform mixture of 99.5 mol% DOPC and 0.5 mol% Rh-DPPE, by following the standard electroformation protocol (18). A thin film of the lipid mixture was deposited on the ITO-coated glass, and dried overnight under vacuum. The electroformation chamber was assembled by two ITO-coated coverslips with the conductive sites facing each other, and separated by a 3 mm thick teflon gasket. For the electro-swelling of GUVS, the chamber was filled with 0.3 M solution of sucrose, and connected to a sinusoidal AC electric field of frequency 10 Hz and amplitude 1.7 V peak-to-peak for 90 minutes. The freshly formed GUV suspension was further diluted in 0.3 M glucose, as required by the experiment.

SLB patches were obtained by diluting GUVs in fusogenic Tris buffer in a ratio 1:10, and fusing them to pre-cleaned microscope slides. The composition of the TRIS buffer was 10 mM Tris.HCl, 150 mM NaCl, 2 mM CaCl2, adjusted to pH $\approx$ 7.5 with 1 M NaOH. Glasses were pre-cleaned by subsequent 10 min sonication in acetone, ethanol and water and were hydrophilised by plasma treatment prior to the bilayer deposition.

CSLB were prepared using the standard SUV fusion method. Briefly, 25 µL of lipid solution (DOPC and Rh-DPPE in a 99.5/0.5 mol % ratio) was dried on the walls of a glass vial overnight and rehydrated in 2 mL Tris buffer (composition as above). The resulting turbid suspension was sonicated with a probe sonicator (Branson) for 10 min at 40% power to obtain small unilamellar vesicles (SUV). The SUVs were diluted further in the TRIS buffer at a ratio of 5:1 and immediately deposited on pre-cleaned coverslip glass. After incubation for about 30 min, the unfused vesicles were removed by carefully washing the glasses with water.

Experimental setup and image analysis

For the experiments, MβCD-Chol (with molar ratio of 1:6 cholesterol: MβCD) and MβCD were diluted in DI water at concentrations between 2 and 50 mg/ml. For the GUV experiments, the osmolarity of the cyclodextrin solutions was adjusted by glucose to protect the vesicles from osmotic shock.

The CSLB and the SLB patches were enclosed in homemade PDMS channels of dimensions $l = 1$ cm, $w = 2$ mm $h = 1$ mm. The cyclodextrin solutions were introduced in the channel via a micro-syringe

pump (Harvard Apparatus) at a flow rate of about 10 µL/min. This resulted in a flow with an average speed of 5 mm/min, which had negligible effects on the bilayer integrity and transformations. The pump was stopped after the chamber was filled with the solution.

For the GUVs experiments, a desired amount of the vesicle suspension was injected into the MβCD-Chol or MβCD solution and carefully mixed to achieve a final concentration of 2 or 10 mg/ml MβCD-Chol. The density difference between the inner sucrose and outer glucose solutions drove the sedimentation of the GUVs to the bottom of the chamber where they were imaged.

The membrane transformations during and after the injection of MβCD-Chol and MβCD solutions were imaged using an inverted confocal laser scanning (Leica Microsystems) microscope. The time interval for image acquisition varied between 0.28-2 s, depending on the speed of the membrane transformations. For the image analysis we used ImageJ. The error bars are calculated as the standard error from five independent experimental measurements.

RESULTS

SLB patches

We first present measurements on SLB patches, which allow us to quantitatively analyze the dynamics of cholesterol transfer from MβCD-Chol to the membrane. The SLB patches remain unaltered under quiescent conditions and constant temperature. However, upon exposure to MβCD-Chol solution of various concentrations, the SLB patches can undergo an area expansion of up to 50% in the first 10 to 50 s, followed later by contraction (Fig. 2-A and B).

We attribute the expansion of the patch solely to the absorption of cholesterol in the membrane. Thus, from the experimentally tracked area changes of the patch, $\Delta a = (A - A_0)/A_0$, where A and A_0 are the actual and initial patch areas (Fig. 2-B), we are able to calculate the cholesterol area fraction $\phi(t)$ in the bilayer as a function of time (see Supplementary materials, Eqs. S1, S2 and S3). For this calculation, we need to know the average area per molecule of the binary DOPC-cholesterol lipid bilayer, which decreases as the cholesterol mole fraction increases. The decrease is on the one hand due to the well-known condensing effect, which arises from the ability of cholesterol to modify the orientation of the phospholipid hydrocarbon chains and decrease the DOPC spacing (19). On the other hand, a cholesterol molecule inserted into a bilayer has a smaller area than DOPC, which results in a smaller total average area per molecule (Fig. S1). To account for the cholesterol condensing effect, we use the experimental data and method given in reference (20) for DOPC SLB patches (Eq. S3).

To a first approximation, the kinetics of cholesterol adsorption can be modelled with a first-order rate equation,

$$\frac{d\phi}{dt}(x,t) = \frac{1}{\tau}\left(\bar{\phi} - \phi(x,t)\right),$$

where τ is the adsorption rate and $\bar{\phi}$ is the cholesterol area fraction at saturation. Under the assumptions that the concentration C of the MβCD-Chol solution above the membrane remains constant everywhere in the buffer, and that the cholesterol is uniformly distributed in the membrane (both laterally and across the leaflets - see Discussion), the solution of the above equation is $\phi(t) = \bar{\phi}(1 - e^{-t/\tau})$, where $\bar{\phi}$ and τ are functions of C. If the adsorption were to follow a simple Langmuir model, the constants of the first-order rate equation will be linearly dependent on C as $1/\tau = k_d + k_a C$, and $\bar{\phi} = \phi^{\max}/(1 + k_d/k_a C)$, where k_d and k_a are desorption and adsorption rate constants, respectively, and $\phi^{\max}$ is the maximum limit of the cholesterol area fraction in the membrane.

As shown in Fig. 2-C, for lower MβCD-Chol concentrations (2, 5, 10 mg/mL) the Langmuir prediction for τ and $\bar{\phi}$ fit perfectly our experimental measurements. Furthermore, using the Langmuir model we find that the maximum limit for the cholesterol area fraction in DOPC membranes is $\phi^{\max} = 0.61$, equivalent to the cholesterol mole fraction of $\chi = 0.68$ (see Eq. S2 for calculations), which is in agreement with previous estimates based on different methods ($\chi = 0.60$ (19), $\chi = 0.67$ (21)).

The deviation from the Langmuir adsorption isotherm at high concentrations of MβCD-Chol can be clearly illustrated by comparing the experimentally measured and theoretically predicted area changes of the patch (Fig. 2-D). Whereas at 2 mg/mL of MβCD-Chol the experiment and the model perfectly agree, the expansion measured at 50 mg/mL MβCD-Chol appears partially slowed down. We propose that this is due to the membrane-substrate friction that becomes increasingly pronounced during fast expansions (i.e. large MβCD-Chol concentrations), as our recent work on membrane patches has suggested (22).

The Langmuir model does not account for the later contraction of the patch area either. The microscopic images reveal that the contraction proceeds as a gradual disintegration of the newly expanded membrane area, resulting in a contracted patch with almost identical contour as the initial one (Fig. 2-A). The likely mechanism of this process is explained in the Discussion.

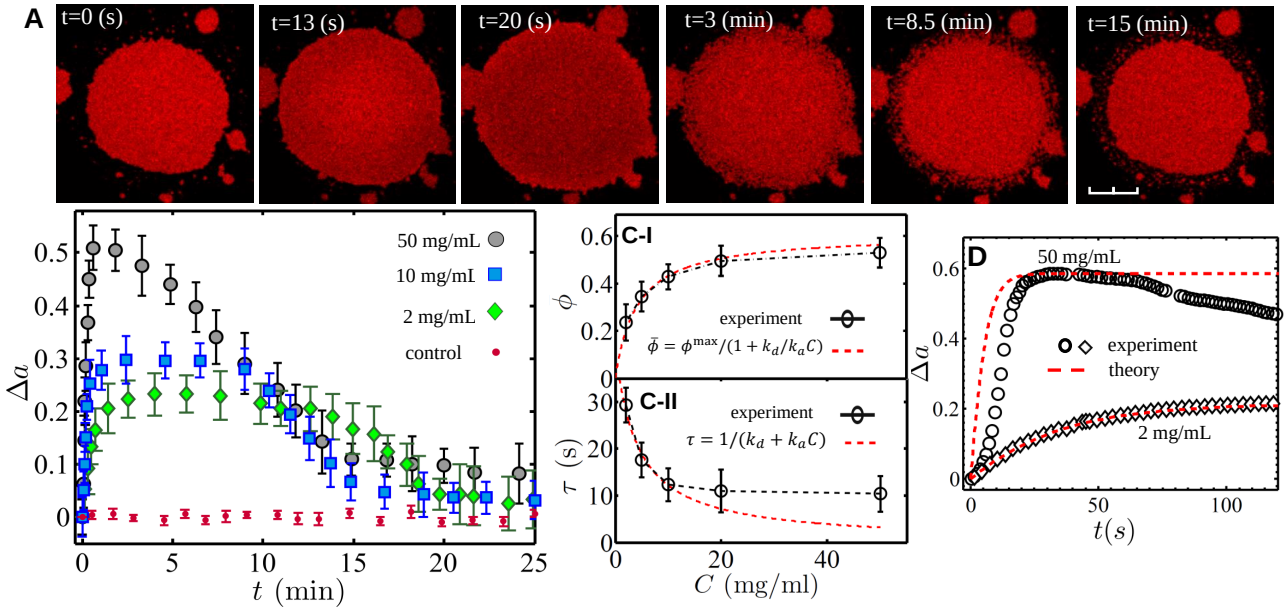

Figure 2: Dynamical transformations of SLB patches upon cholesterol adsorption. (A) Confocal images of a patch exposed to 50 mg/mL MβCD-Chol solution. Scale bar: 10 µm. (B) Normalized area deviation of SLB patches $\Delta a = (A - A_0)/A_0$ versus time for several concentrations. We set $t = 0$ s as the onset of expansion for each experiment. (C) Steady state cholesterol area fraction $\bar{\phi}$ and the expansion relaxation time τ during cholesterol adsorption as functions of the MβCD-Chol concentration. Experimental data are fitted with Langmuir adsorption isotherm for low concentrations ($C = 2$, 5, 10 mg/mL), resulting in the Langmuir adsorption constants $k_a = 0.0058$ mg/(mL·s), $k_d = 0.024$ 1/s, $\phi^{\max} = 0.61$. (D) Normalized area change of the SLB patch during the expansion, measured experimentally and predicted from a uniform Langmuir adsorption model for $t = 0 - 120$ s.

Continuous Supported Lipid Bilayer

Next, we consider a continuous supported lipid bilayer (CSLB) system, which better mimics the lipid continuity of the cell membrane and its confinement to the cytoskeleton or extracellular matrix. Our experiments reveal that exposure of CSLBs to MβCD-Chol results in the growth of multiple out-of-plane lipid tubules (Fig. 3-A). These tubes are unstable, particularly at higher concentrations of MβCD-Chol solution, and quickly collapse into multilamellar globules that shrink gradually with time.

The response of the CSLB to transient cholesterol uptake can be intuitively understood as a result of excess surface area in a laterally constrained lipid bilayer. In contrast to the membrane patch, the CSLB does not have space to expand laterally and upon absorption of cholesterol it releases the excess area as out-of-plane membrane protrusions. This analogy is confirmed by our analysis of the time-dependent variations in the fluorescent intensity (FI) of the CSLB (the supported part), as the non-fluorescent cholesterol gets absorbed (Fig. 3-B). For comparison, the FI of a control CSLB exposed to water remains constant throughout the imaging period. Assuming that the cholesterol and the fluorescently labelled lipids (Rh-DPPE) are uniformly distributed in the membrane and that the bilayer is inextensible, $FI \propto n_{Rh-DPPE}/A$, where $n_{Rh-DPPE}$ is the number of Rh-DPPE molecules, and A is the total area of the CSLB (supported part and area in the protrusions). Since $n_{Rh-DPPE}$ is unaffected by the MβCD-Chol solution, we can write $FI/FI_0 = A/A_0$, where FI_0 is measured at $t = 0$ s. Hence, the excess surface area arising from the absorption of cholesterol and driving the formation of protrusions can be obtained as $\Delta a \approx FI_0/FI - 1$. The results in Fig. 3-B show the excess surface area in CSLBs follows a very similar dynamics to the one measured with membrane patches, both as a function of time and of MβCD-Chol concentration. The increase and consequent decrease observed experimentally coincide respectively with the formation and the collapse of the supported bilayer protrusions.

GUVs

Whereas CSLBs release their excess surface area through discrete membrane protrusions to limit detachment from the substrate (23), the free standing membranes of giant unilamelar vesicles (GUVs) have been

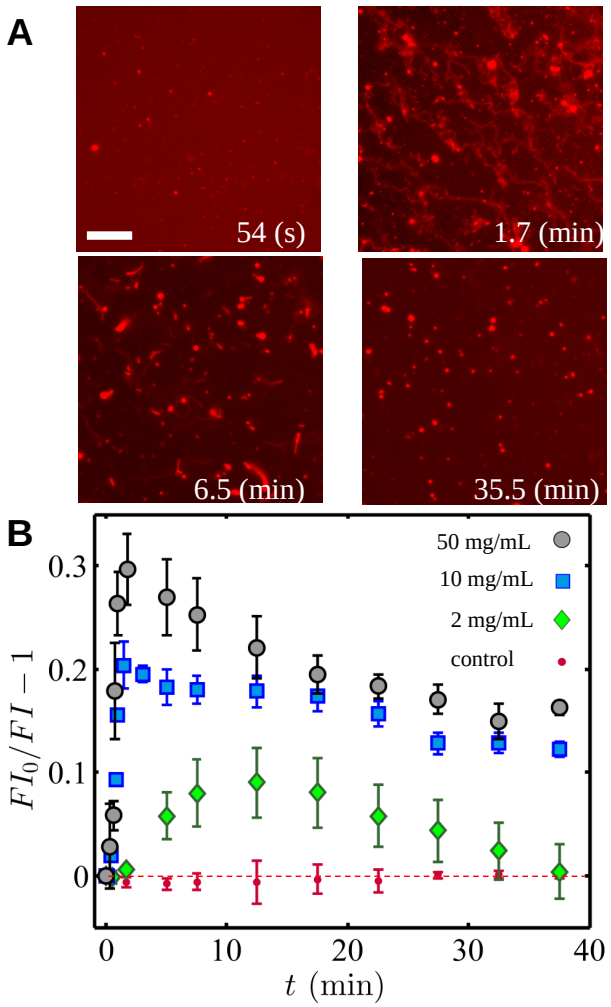

Figure 3: Response of CSLB to MβCD-Chol solution. (a) Confocal images of the formation and evolution of tubular protrusions from CSLB upon exposure to 10 mg/mL of MβCD-Chol. Scale bar is 20 µm. (b) The average changes in the excess surface area of CSLBs obtained as $FI_0/FI - 1$ for several MβCD-Chol concentrations. The control measurements on lipid bilayer exposed to water and a linear fit to them are shown in red.

shown to respond by large-scale fluctuations and eventually outward budding (24, 25). In our experiments with MβCD-Chol, GUVs do initially respond to cholesterol uptake by an increase in their surface area and enhanced membrane fluctuations, but to our surprise they also form multiple inward tubes, which fill the vesicle interior (Fig. 4). This response is much more pronounced at higher MβCD-Chol concentrations and can even lead to vesicle collapse. Similar to the observations on the supported membranes, at later times the GUV surface area decreases, as demonstrated by the decrease in the

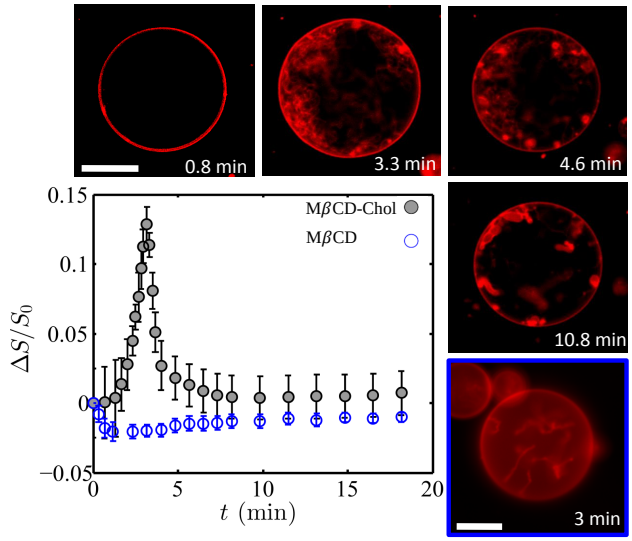

Figure 4: GUV response to 2 mg/mL MβCD-Chol and 2 mg/mL MβCD solutions. A representative plot of the changes of the normalized spherical surface area of GUVs obtained by measuring the equatorial perimeter P, i.e. $\Delta S/S_0 = (\Delta P/P_0)^2$. The unframed confocal images show the formation and evolution of the inward vesicle protrusions in MβCD-Chol solution, whereas the image framed in blue shows the corresponding vesicle transformations in MβCD solution. Scale bar is 20 µm.

vesicle perimeter and the shrinking of the tubes into intra-vesicle buds (Fig. 4).

Effects of MβCD on phospholipid membranes

Intrigued by the unexpected membrane responses to MβCD-Chol that cannot be ascribed solely to the uptake of cholesterol, namely the formation of protrusions inside the vesicles and the contraction of patches and SLB protrusions, we tested the effects of empty cyclodextrins (MβCD) on lipid bilayers. MβCD is widely used to deplete lipid and cell membranes of cholesterol (14, 26). Our MβCD-Chol solutions contain a certain fraction of empty cyclodextrin (as prescribed by the manufacturer), which further grows as the MβCD-Chol delivers cholesterol to the lipid membrane.

Our results show that empty cyclodextrins may indeed explain some of the effects occurring at the later stages of membrane MβCD-Chol exposure. For example, MβCD alone induces inward tubes in GUVs, albeit shorter and of smaller density to the one observed with cholesterol-loaded cyclodextrin (Fig. 4). Similar moderate amounts of MβCD do not cause shape changes in supported lipid bilayers, but can increase the FI of CSLBs above the control levels similar to the increase

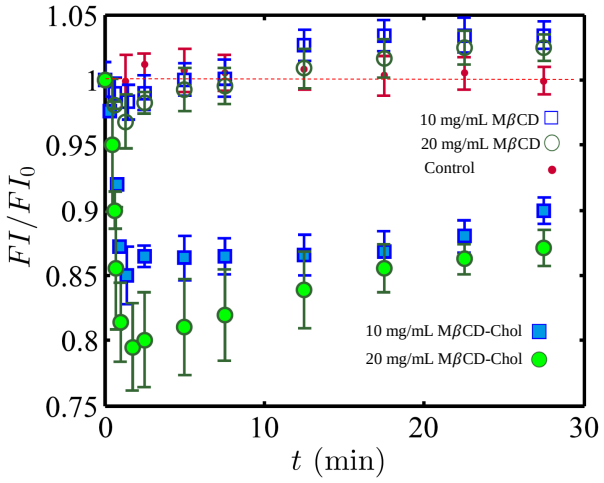

Figure 5: Change in the relative fluorescent intensity (FI/FI_0) of Rhodamine labeled SLBs to 10 and 20 mg/mL MβCD and MβCD-Chol. The control measurements on a lipid bilayer exposed to water and a linear fit to them are shown in red.

observed following exposure to MβCD-Chol (Fig. 5). At high concentrations, the MβCD is able to disintegrate the bilayer, as witnessed by the formation of pores in CSLB (Fig. S2), the disappearance of SLB patches (Fig. S3) or the bursting of GUVs (images not shown).

DISCUSSION

In this section, we reconcile the variety of observations from our experiments and discuss their mechanisms. Cholesterol is a small amphiphilic molecule and its flip-flop rate is expected to be very fast, as the majority of studies show (27, 28). Thus upon its transfer from the MβCD-Chol donor to the membrane, cholesterol would distribute uniformly across the lipid bilayer, and the initial transformations of our membrane systems, namely the expansion of the SLB patches (Fig. 2-A,B), the formation of tubes in CSLBs (Fig. 3-A) and the increased fluctuations in GUVs (Fig. 4), are consistent with an excess membrane area gained upon cholesterol uptake.

It must be noted that formation of tubes in supported bilayers has been previously observed as a result of an asymmetric insertion of peptides, fatty acids, surfactants or polysacharides (29–32). Slow cholesterol flip-flop rate, as suggested by some studies (33), may indeed result in a transient cholesterol asymmetry and a positive spontaneous membrane curvature. However it would also cause formation of outward tubes in GUVs (34), which obviously contradicts our results. Cholesterol asymmetry arising only in supported membrane systems has been excluded by the recent study of Liu et al., who show using sum frequency vibration spectroscopy that the membrane support does not influence the cholesterol flip flops (33). Thus we conclude that the uniform increase in the lipid density following cholesterol uptake is the most likely mechanism for the formation of tubes in continuous supported bilayers. The latter is supported by our analogous findings with mechanically strained CSLBs (23, 35). A similar mechanism is very likely to play a role in biological membranes (continuous and actin-supported), as demonstrated by a recent study on adherent cells subject to mechanical compression (36).

Following the initial uptake of cholesterol, we observe a decrease in the membrane surface area in all three model systems, evidenced by patch contraction, shrinking of membrane protrusions in CSLBs or decrease in the GUV radius. Given its late onset, the membrane contraction is unlikely to be caused by the cholesterol condensing effect. In fact, we have accounted for the cholesterol condensation when modelling the membrane area expansion dynamics (SI). We believe instead that the membrane contraction is an artefact of the cholesterol donor system, caused by the empty cyclodextrin in the MβCD-Chol solution. In addition to its main application for cholesterol depletion, MβCD have also been shown to extract phospholipids from lipid membranes, though at longer time scales (14, 26, 37) (see SI). This is confirmed by our results showing an increase in the FI of CSLBs after exposure to both MβCD and MβCD-Chol solutions (Fig. 5) (we expect that cyclodextrin extracts DOPC but not Rhodamine-labeled DOPC due to the large size of the flurophore). Moreover, the depletion of DOPC from the outer membrane leaflet of GUVs and the resulting negative spontaneous curvature may also explain the formation of inward tubes in this system (Fig. 4).

Our experiments suggest further that the extraction of phospholipids by cyclodextrin is not homogeneous across the membrane. Firstly, free standing membranes of GUVs or membrane protrusions appear much more susceptible to lipid depletion than the substrate-supported membranes. The latter get affected by MβCD, only at very high concentrations or after long exposure times (Fig. S2 and S3). Secondly, shortly after the expansion of the patches, the membrane in the expansion annulus disintegrates completely and the patch assumes its original shape (Fig. 2-A). This leads us to the suggestion that the newly expanded membrane has a weaker coupling to the substrate then the original patch and therefore is more susceptible to DOPC removal by the empty cyclodextrin. The reasons for this response can be ascribed to the compositional differences between the cyclodextrin solution and the fusogenic buffer, which is used to prepare the supported membranes. As shown in the SI, cyclodextrin can adsorb

onto the hydrophilic glass and membranes formed on cyclodextrin-covered glasses appear more unstable than membranes formed on clean glasses. The absence of ions in the cyclodextrin solution may also have an effect.

CONCLUSIONS

In summary, we have shown that rapid cholesterol uptake is able to induce significant morphological transformations in lipid membranes. By using MβCD-Chol as a cholesterol donor and model lipid membrane systems under different geometric constraints, we have shown a variety of responses resulting from the interplay of mechanical and chemical mechanisms. For example, 1-20 mM MβCD-Chol solution, as typically used on cells (13, 14), delivers cholesterol to lipid membranes within 15-30 s, causing up to a 30% increase in the membrane area. This produces a membrane area expansion (Fig. 2) or the growth of out-of plane membrane protrusions in laterally constrained bilayers (Fig. 3-a). GUVs also form tubes upon MβCD-Chol exposure, though inward, but the tubes are caused predominantly by the ability of emptied cyclodextrins to extract phospholipids of the outer monolayer on a longer time scale.

Our results have significant implications in interpreting the response of cells to cholesterol enrichment. For example, activation of signaling pathways in cells and cytoskeletal remodeling observed after incubating cells with MβCD-Chol (6, 7, 38, 39) are likely triggered by the non-specific increase in the membrane area, and thus a decrease in membrane tension, rather than by cholesterol itself. This suggestion is supported by recent studies that demonstrate the strong interplay between the membrane tension and the remodeling of the cell membrane and cytoskeleton (36, 40, 41). Finally, our work shows that MβCD-Chol should be used with caution as a cholesterol donor in cell and synthetic membrane studies, as the cyclodextrin may also extract a significant amount of phospholipids, thus inducing a variety of unexpected membrane responses, the mechanisms of which would require further investigation.

SUPPLEMENTARY MATERIAL

An online supplement to this article can be found by visiting BJ Online at http://www.biophysj.org.

Author Contributions

M.R., D.R., A.B.S. and M.S. performed the experiments, M.R., M.A. and H.A.S. did the theoretical modelling, M.S., M.R., M.A., H.A.S. and A.B.S. wrote the manuscript.

ACKNOWLEDGMENTS

M.R., M.S. and H.A.S. thank Princeton University and M.S. thanks the Biophysical Science Institute at Durham University for financial support. M.R. and M.A. acknowledge the support of the European Research Council (FP7/2007-2013, grant Nr 240487) and A.B.S. acknowledges the support of NSF Award Number CBET-1512686. J. Girkin is acknowledged for imaging support, and J. M. Vanegas for helpful discussions.

References

[1] Ikonen, E., 2008. Cellular cholesterol trafficking and compartmentalization. Nat. Rev. Mol. Cell Biol. 9:125–138.

[2] Maxfield, F. R., and D. Wüstner, 2002. Intracellular cholesterol transport. J. Clin. Invest. 110:891–898.

[3] Tabas, I., 2002. Consequences of cellular cholesterol accumulation: basic concepts and physiological implications. J. Clin. Invest. 110:905–912.

[4] Maxfield, F., and I. Tabas, 2005. Role of cholesterol and lipid organization in disease. Nature 438:612–621.

[5] Nagao, T., C. Qin, I. Grosheva, F. R. Maxfield, and L. M. Pierini, 2007. Elevated cholesterol levels in the plasma membranes of macrophages inhibit migration by disrupting RhoA regulation. Arterioscler Thromb Vasc Biol. 27:1596–1602.

[6] Grosheva, I., A. Haka, C. Qin, L. Pierini, and F. Maxfield, 2009. Aggregated LDL in contact with macrophages induces local increases in free cholesterol levels that regulate local actin polymerization. Arterioscler Thromb Vasc Biol. 29:1615–1621.

[7] Qin, C., T. Nagao, I. Grosheva, F. Maxfield, and L. Pierini, 2006. Elevated plasma membrane cholesterol content alters macrophage signaling and function. Arterioscler Thromb Vasc Biol. 26:372–378.

[8] Simons, K., and W. Vaz, 2004. Model systems, lipid rafts, and cell membranes 1. Annu. Rev. Biophys. Biomol. Struct. 33:269–295.

[9] Lange, Y., J. Ye, and T. L. Steck, 2004. How cholesterol homeostasis is regulated by plasma membrane cholesterol in excess of phospholipids. Proc. Natl. Acad. Sci. U.S.A. 101:11664–11667.

[10] Simons, K., and D. Toomre, 2000. Lipid rafts and signal transduction. Nat. Rev. Mol. Cell Biol. 1:31–39.

[11] Kwik, J., S. Boyle, D. Fooksman, L. Margolis, M. Sheetz, and M. Edidin, 2003. Membrane cholesterol, lateral mobility, and the phosphatidylinositol 4, 5-bisphosphate-dependent organization of cell actin. Proc. Natl. Acad. Sci. U.S.A. 100:13964–13969.

[12] Varsano, N., I. Fargion, S. G. Wolf, L. Leiserowitz, and L. Addadi, 2015. Formation of 3D Cholesterol Crystals from 2D Nucleation Sites in Lipid Bilayer Membranes: Implications for Atherosclerosis. J. Am. Chem. Soc. 137:1601–1607.

[13] Christian, A., M. Haynes, M. Phillips, and G. Rothblat, 1997. Use of cyclodextrins for manipulating cellular cholesterol content. J. Lipid Res 38:2264–2272.

[14] Zidovetzki, R., and I. Levitan, 2007. Use of cyclodextrins to manipulate plasma membrane cholesterol content: evidence, misconceptions and control strategies. Biochimica et Biophysica Acta (BBA)-Biomembranes 1768:1311–1324.

[15] Brasaemle, D. L., and A. D. Attie, 1990. Rapid intracellular transport of LDL-derived cholesterol to the plasma membrane in cultured fibroblasts. J. Lipid Res 31:103–112.

[16] Johnson, W. J., G. K. Chacko, M. C. Phillips, and G. H. Rothblat, 1990. The efflux of lysosomal cholesterol from cells. J. Biol. Chem. 265:5546–5553.

[17] Jiang, D., A. Devadoss, M. S. Palencsár, D. Fang, N. M. White, T. J. Kelley, J. D. Smith, and J. D. Burgess, 2007. Direct electrochemical evaluation of plasma membrane cholesterol in live mammalian cells. J. Am. Chem. Soc. 129:11352–11353.

[18] Angelova, M., and D. Dimitrov, 1986. Liposome electroformation. Faraday Discuss. Chem. Soc. 81:303–311.

[19] Hung, W., M. Lee, F. Chen, and H. Huang, 2007. The condensing effect of cholesterol in lipid bilayers. Biophys. J. 92:3960–3967.

[20] Litz, J. P., N. Thakkar, T. Portet, and S. L. Keller, 2016. Depletion with Cyclodextrin Reveals Two Populations of Cholesterol in Model Lipid Membranes. Biophysical journal 110:635–645.

[21] Ali, M. R., K. H. Cheng, and J. Huang, 2007. Assess the nature of cholesterol–lipid interactions through the chemical potential of cholesterol in phosphatidylcholine bilayers. Proc. Natl. Acad. Sci. U.S.A. 104:5372–5377.

[22] Stubbington, L., M. Arroyo, and M. Staykova, In Press-2016. Sticking and sliding of lipid bilayers on deformable substrates. Soft Matter .

[23] Staykova, M., M. Arroyo, M. Rahimi, and H. A. Stone, 2013. Confined Bilayers Passively Regulate Shape and Stress. Phys. Rev. Lett. 110:028101.

[24] Solon, J., J. Pécréaux, P. Girard, M. Fauré, J. Prost, and P. Bassereau, 2006. Negative tension induced by lipid uptake. Phys. Rev. Lett. 97:98103.

[25] Sudbrack, T. P., N. L. Archilha, R. Itri, and K. A. Riske, 2010. Observing the solubilization of lipid bilayers by detergents with optical microscopy of GUVs. J. Phys. Chem. B 115:269–277.

[26] Huang, Z., and E. London, 2013. Effect of Cyclodextrin and Membrane Lipid Structure upon Cyclodextrin–Lipid Interaction. Langmuir 29:14631–14638.

[27] Bennett, W., J. MacCallum, M. Hinner, S. Marrink, and D. Tieleman, 2009. Molecular view of cholesterol flip-flop and chemical potential in different membrane environments. J. Am. Chem. Soc. 131:12714–12720.

[28] Hamilton, J. A., 2003. Fast flip-flop of cholesterol and fatty acids in membranes: implications for membrane transport proteins. Curr. Opin. Lipidol. 14:263–271.

[29] Domanov, Y., and P. Kinnunen, 2006. Antimicrobial peptides temporins B and L induce formation of tubular lipid protrusions from supported phospholipid bilayers. Biophys. J. 91:4427–4439.

[30] Thid, D., J. Benkoski, S. Svedhem, B. Kasemo, and J. Gold, 2007. DHA-induced changes of supported lipid membrane morphology. Langmuir 23:5878–5881.

[31] Khalifat, N., M. Rahimi, A.-F. Bitbol, M. Seigneuret, J.-B. Fournier, N. Puff, M. Arroyo, and M. I. Angelova, 2014. Interplay of packing and flip-flop in local bilayer deformation. How phosphatidylglycerol could rescue mitochondrial function in a cardiolipin-deficient yeast mutant. Biophys. J. 107:879–890.

[32] Yoon, B. K., J. A. Jackman, M. C. Kim, and N.-J. Cho, 2015. Spectrum of membrane morphological responses to antibacterial fatty acids and related surfactants. Langmuir 31:10223–10232.

[33] Liu, J., K. L. Brown, and J. C. Conboy, 2013. The effect of cholesterol on the intrinsic rate of lipid flip–flop as measured by sum-frequency vibrational spectroscopy. Faraday discussions 161:45–61.

[34] Lipowsky, R., 2013. Spontaneous tubulation of membranes and vesicles reveals membrane tension generated by spontaneous curvature. Faraday Discuss 161:305–331.

[35] Staykova, M., D. Holmes, C. Read, and H. Stone, 2011. Mechanics of surface area regulation in cells examined with confined lipid membranes. Proc. Natl. Acad. Sci. U.S.A. 108:9084–9088.

[36] Kosmalska, A. J., L. Casares, A. Elosegui-Artola, J. J. Thottacherry, R. Moreno-Vicente, V. Gonzalez-Tarrago, M. A. del Pozo, S. Mayor, M. Arroyo, D. Navajas, N. C. Trepat, X abd Gauthier, and P. Roca-Cusachs, 2015. Physical principles of membrane remodelling during cell mechanoadaptation. Nat. Commun. 6:7292.

[37] Sanchez, S. A., G. Gunther, M. A. Tricerri, and E. Gratton, 2011. Methyl-β-cyclodextrins preferentially remove cholesterol from the liquid disordered phase in giant unilamellar vesicles. J. Membr. Biol. 241:1–10.

[38] Norman, L., R. Oetama, M. Dembo, F. Byfield, D. Hammer, I. Levitan, and H. Aranda-Espinoza, 2010. Modification of cellular cholesterol content affects traction force, adhesion and cell spreading. Cell. Mol. Bioeng. 3:151–162.

[39] Grimmer, S., B. van Deurs, and K. Sandvig, 2002. Membrane ruffling and macropinocytosis in A431 cells require cholesterol. J. Cell Sci. 115:2953–2962.

[40] Gauthier, N. C., M. A. Fardin, P. Roca-Cusachs, and M. P. Sheetz, 2011. Temporary increase in plasma membrane tension coordinates the activation of exocytosis and contraction during cell spreading. Proc. Natl. Acad. Sci. U.S.A. 108:14467–14472.

[41] Batchelder, E. L., G. Hollopeter, C. Campillo, X. Mezanges, E. M. Jorgensen, P. Nassoy, P. Sens, and J. Plastino, 2011. Membrane tension regulates motility by controlling lamellipodium organization. Proc. Natl. Acad. Sci. U.S.A. 108:11429–11434.